Scientific paper

Foil-based TiO_2/gel Electrolyte/$Ni_{1-x}O$ Electrochromic Device Made of Electrochromic Pigment Coatings

Mohor Mihelčič,[1] Angela Šurca Vuk,[1,2] Dejan Vrhovšek,[3] Franc Švegl,[4] Metka Hajzeri[1] and Boris Orel[1,2,*]

[1] *National Institute of Chemistry, Hajdrihova 19, 1000 Ljubljana, Slovenia*

[2] *CO-NOT, Hajdrihova 19, Ljubljana, Slovenia*

[3] *Cinkarna d.d., Kidričeva 26, 3001 Celje, Slovenia*

[4] *Amanova Ltd., Tehnološki Park 18, 1000 Ljubljana, Slovenia*

** Corresponding author: E-mail: boris.orel@ki.si*
Phone: 00386-(0)1-4760-276; Fax: 00386-(0)1-4760-300

Received: 24-12-2013

Dedicated to the memory of Prof. Dr. Marija Kosec.

Abstract

Thin electrochromic coatings were obtained by co-grinding the mTiA particle aggregates (300 nm in size) with open-corner heptaisobutyl trisilanol POSS (T_8 IB_7 $(OH)_3$ POSS) acting as dispersant. After the addition of titanium tetraisopropoxide (3–5%) the mTiA pigment dispersion was deposited on FTO glass and plastic ITO PET foils and coatings were obtained by thermal treatment at 150 °C.

Optical transmittance and luminous haze from 2 to 6% of the coatings were determined from the corresponding UV-Vis spectra. The achieved electrochromic effect was evaluated by electrochemical charging/discharging in 1 M $LiClO_4$/PC electrolyte. Results revealed that the colouring/bleaching changes depended on the extent of grinding and the size of the milling zirconia beads, enabling to distinguish between the surface charging of the mTiA grains and the filling and emptying of the anatase density of states.

mTiA pigment coatings deposited on plastic foil were used in combination with $Ni_{1-x}O$ pigment coatings for construction of foil-based electrochromic device employing novel gel electrolyte with ionic liquid co-solvent.

Keywords: TiO_2, anatase, pigment coatings, electrochromics, flexible electrochromic device, gel electrolyte.

1. Introduction

Glass based electrochromic (EC) devices providing light transmittance modulation have been extensively studied in the past because of their potential for manufacturing "smart" windows for buildings.[1] Recently foil-based EC devices[2–6] attracted attention (Fig. 1), because they can be made from coatings deposited by highly efficient deposition techniques such as wet roll-to-roll (R2R) processing,[7] spray-coating, spin-coating, inkjet printing and vacuum based R2R deposition.[6,8] Among them roll-to-roll technique process having high potential for production of commercial "smart" windows at a price up to 10–50 times lower (~50 \$/m^2 for a whole EC stack[9]) as compared to the standard glass-based EC windows.[9,10] When suitable pigment dispersions (i.e. paints) are available, wet R2R (i.e. coil-coating) application technique enables mass production of many different functional coatings; spectrally selective paint coating based on black spinel pigments for aluminium-based solar absorbers[11–14] are typical solar energy related products. Large and commercially important field of application is inkjet printing enabling the fabrication of coatings used in many electronic devices and systems. Surface tension, rheological properties, stability of pigment dispersions and size of dispersed pigment particles, all of them should be known in details and taken into account in or-

der to deposit functional coatings by any of the mentioned wet deposition techniques.[15]

A simple and robust wet-deposition process similar to that used for paint production has been developed in our laboratory[16–19] and its efficacy has been demonstrated by deposition of electrochromic $Ni_{1-x}O$ coatings from dispersions made of pre-prepared $Ni_{1-x}O$ pigment dispersed with nickel oxyhydroxyde (NiO_xH_y). The appropriateness of $Ni_{1-x}O$ pigment dispersions coil-coating deposition has been demonstrated on coil-coating line in Coatema factory in Germany (www.coatema.de) in the frame of EU project INNOSHADE (www.innoshade.eu). This led us to transfer the knowledge[17,18] to the deposition of optically transparent TiO_2 pigment coatings based on metatitanic acid (anatase) powder (mTiA, for short)[20] on conductive foils.

Therefore, the goal of this study was to provide evidences that wet deposition of mTiA pigment dispersions (i.e. paint) could bring about pigment coatings with low scattering of visible light (i.e. low haze) and showing also strong EC effect. Namely, in our preliminary study,[21] commercial TiO_2 (anatase) pigment manufactured by Cinkarna Factory (SI) with ill-defined structure and composition was used. The metatitanic acid pigment dispersions were made by milling the pigment with the help of open-corner heptaisobutyl POSS-triol (T_8 IB_7 $(OH)_3$ POSS, trisilanol POSS, for short) dispersant, which enabled the deposition of pigment coatings having low haze (up to 6%). Among many commercial titania pigments, mTiA was selected because the EC properties of mTiA pigment coatings have not been reported yet and the material is easily made in a form of bare pigment particles, without any additional surface modifying layer.

We expected to get information about the EC effect inherent to the mTiA pigment coatings, and to compare it with other titania based EC coatings; compacted powders of anatase heat-treated at 750 °C,[22,23] mixed anatase and rutile coarse particle-like coatings made by anodic spark deposition technique reported by Reinhardt et al.,[24] sintered EC titania coatings deposited by doctor blade technique,[25] titania coatings used for reflective EC devices (usually with adsorbed viologens)[26,27] and many studies of titania coatings developed for dye-sensitized photoelectrochemical (DSPEC)[28] and photoelectrochromic (PEC) cells.[29]

It should be noted that TiO_2 pigment coatings for EC applications share certain common problems with those used for PEC and DSPEC devices, also consisting of pigment particles, but strongly differ in others. Good particle-to-particle and particle-to-substrate contacts should be attained already at low processing temperatures (i.e., ITO PET is stable up to T < 150 °C.[4]). Organic polymeric resin binders, which are usually employed for making sintered nanocrystalline TiO_2 photoanodes for PEC and DSPEC and fill the voids between particles therefore hindering the insertion of lithium ions into the particle based EC coatings, must be avoided. Thus, titainum tetraisopropoxide ($Ti(iOPr)_4$) was used as a binder (up to 20%) in order to assure mechanical integrity of the mTiA pigment coatings. $Ti(iOPr)_4$ was perfectly suitable as a binder because it forms compact films already at low temperatures and is compatible with the mTiA pigment. In general terms, mTiA electrochromic pigment coatings are basically sol-gel based coatings made of sol-gel pigment dispersion.

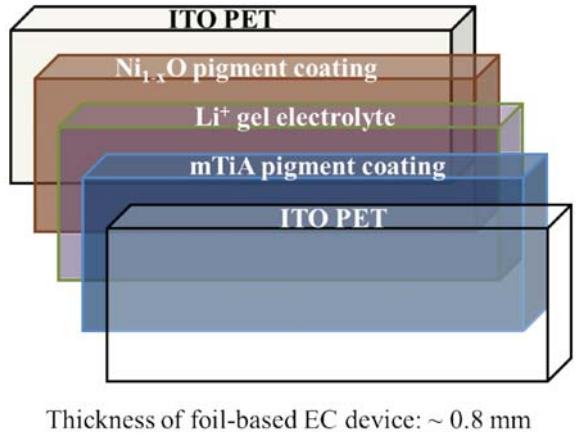

Fig. 1. Schematic presentation of foil-based EC device, consisting of $Ni_{1-x}O$ pigment coating/mTiA02 pigment coating, glued together with Li^+ gel (semi-solid) electrolyte.

Additional arguments substantiating more detailed studies of EC properties of mTiA are of general importance, originating from the fact that TiO_2 is not very popular EC material and during the last four decades nanoparticles of TiO_2 and thin films attracted only a sporadic interest in research devoted to electrochromism.[1] TiO_2 has been recognized as cathodically colouring material, which darkens under double insertion of ions and electrons, even though some studies have shown that TiO_2 can act also as non-colouring (i.e. optically passive) coating (for example, CeO_2/TiO_2 sol-gel films).[30–32] Thin TiO_2 film have been made with various techniques: evaporation,[33] sputtering and also with wet-deposition techniques such as anodization,[37] chemical bath deposition (CBT) technique[38] and sol-gel technique.[39,40] The latter techniques usually require heat-treatment of colloidal solutions at temperatures from 350–450 °C in order that anatase particles form *in-situ*. This means that wet deposition of coatings from pigment dispersions represent the most suitable approach for making pigment coatings for foil-based EC devices.

Electrochromic properties of titania coatings as reviewed by Sorar at al.[41] strongly depend on the preparation technique, which substantiated the assessment of EC properties also for the mTiA pigment coatings deposited from paints. For example, sputtered films show coloration efficiency η from 5 up to 37 cm^2/C,[35–36] while early works on sol-gel deposited films even claim TiO_2 films as grey colouring films.[42] Ozer et al.[43,44] were the first to demon-

strate that large η values could be achieved also with sol-gel technique. Gillet et al.[45] and Ivanova and Harizanova[46] have later shown that the η values for a dense sintered TiO_2 films dropped significantly, while samples comprising TiO_2 nanoparticles exhibit much higher η values. The large effective surface area of TiO_2 particles,[47] expected also to be present in pigment coatings reported in this study, provides a concomitant large number of adsorption sites for intercalation of ions, while the high surface-to-volume ratio ensures minimal diffusion path-lengths. This agrees with results reported by Nang Dinh et al.[25] who have shown that sintered TiO_2 particles deposited on FTO glass by doctor blade technique and consisting of porous and interconnected particles significantly increased ion storage capacity (~60 mC/cm^2 for 600 nm thick coatings), colouring/bleaching changes and stability of the EC effect (85% fading after 500 cycles), but decrease the speed of transmittance variations (few seconds).

It is clear that due to the controlled milling, the mTiA pigment coatings represent well-defined particle system, which was suitable for obtaining correlation between the effect of the size of the particle aggregates formed and the intercalation of lithium ions and concurrent EC effect. The haze of TiO_2 pigment coatings on FTO glass in initial state was determined in the range from 2 to 6%, depending on the coating thickness. On the basis of cyclic voltammograms and *in-situ* UV-Vis spectroelectrochemical measurements the coloration efficiency was assessed, while the onset of colouring and bleaching changes as a function of applied potential, shed light on the role of the pigment particle surface on the insertion/extraction reactions.

In the last part of this study, we demonstrated the EC effect of the mTiA pigment coatings by making EC device, which was constructed in combination with $Ni_{1-x}O$ pigmented coating[17,18] (Fig. 1). As stated by Granqvist et al.,[48] the use of gel or solid state electrolytes is important from many practical reasons, one of the most important ones is to present leakage. Herein, instead of PVC membrane based lithium electrolyte[21] we used an sol-gel electrolyte made of long-chain poly(ethyleneoxide) (M_w ~ 400, $(PEO)_n$ (n = 12)) terminated on both ends by trialkoxysilane groups linked via the uretano groups (urethanosil) to the PEO_{12} chains.[49,50] Lithium bis(trifluoromethanesulfonyl)imide (LiTFSI) served as a source for lithium ions. Haze, considered as one of the most relevant parameters of the pigment coatings, was determined also for EC device and correlated to the haze values shown by the individual pigment coatings.

2. Experimental

2. 1. Materials and Preparation of Coatings

Metatitanic acid powder (mTiA)). mTiA powder was prepared by the so-called "sulfate route"[20] and is currently used for its industrial manufacturing in the Cinkarna d.d. factory (www.cinkarna.si). In brief, white precipitate mTiA is obtained after dissolution of ilmenite in concentrated suphuric acid (98%, Cinkarna Celje), hydrolyzed in the presence of anatase seeds. The anatase seeds were prepared separately by hydrolyzing a titanyl sulphate solution at 80 °C and are added into dissolved ilmenite solution. By the variation of the amount of the solution (from 0.1–1.8%) different mTiA types are easily produced differing in the size of anatase powder.

From the XRD analysis of the mTiA powder milled in the presence of trisilanol POSS (Fig. 2) it was conceived that the pigment consisted of mixed rutile (~15%) and anatase phase.[20] The mTiA crystallites were composed of nanoparticles, which size was estimated from the various (hkl) peaks (A(101), A(004), A(200) and A(105)) to about 5–7 nm. They formed larger aggregates (up to 20–50 nm in size). Expectedly, the presence of trisilanol POSS was not observed. Such structure of the mTiA pigment aggregates was also obtained from TEM measurements (not shown here).

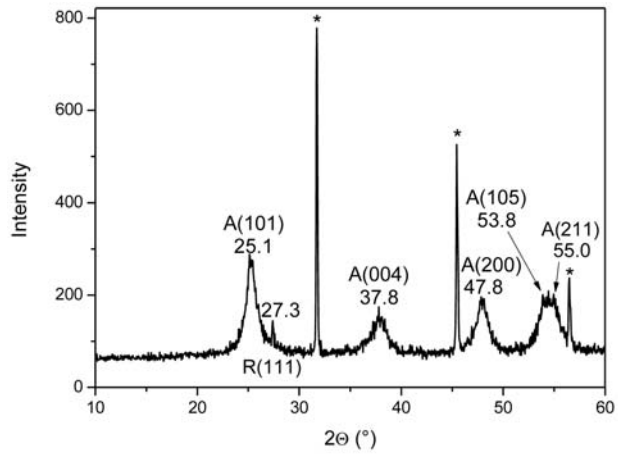

Fig. 2. XRD of trisilanol POSS/mTiA powder milled with zirconia beads (0.2 mm) with indicated (hkl) peaks and the corresponding 2Θ values. A corresponds to anatase and R to rutile phase; reflections of Al holder are indicated by *.

mTiA agglomerates (size up to few μm) consist of aggregates, the size of which is from 30–50 nm. The aggregates are formed of nanocrystallites (5–8 nm in size), determined from the XRD analysis of the mTiA powder (Fig. 2), strongly linked together via the crystalline bridges. In order to obtain dispersed aggregates of mTiA powder a small amount of barium chloride was added to the mTiA agglomerates.[20] Since barium has high affinity towards sulphate ions, the added barium salt drew together sulphate ions, which were removed from the mTiA by centrifugation, freeing agglomerates and forming separated aggregates. Before the as-prepared mTiA aggregates were used for making pigment dispersions, mTiA pigment

was thoroughly washed with distilled water and then dried at 100 °C. As-prepared dry mTiA powder aggregates were used for preparation of pigment dispersions.

Beside mTiA pigment, also commercial nanocrystalline TiO_2 obtained from Inframat (TiInfr, for short) and P25 anatase pigment (Degussa, DE) were used for making the pigment dispersions and pigment coatings deposition.

Preparation of pigment dispersion. 10 wt.% of as-prepared mTiA and TiInfr powders were first dispersed in n-butanol (Sigma-Aldrich) in the presence of trisilanol POSS dispersant (10 wt.% vs. powder), while P25 pigment dispersion was prepared by milling of the raw pigment in butanol without addition of any dispersant. The synthesis of trisilanol POSS was reported previously,[12,13] but could be obtained also commercially [www.hybrid plastics.com]. mTiA was milled with zirconia beads with dimensions of 0.4, 0.2 and 0.1 mm providing pigment dispersions mTiA04, mTiA02 and mTiA01, respectively. Since the mTiA02 coatings exhibited the smallest particle size, surface roughness and haze (Table 1), the TiInfr and P 25 pigments were milled only with the zirconia beads with diameter size of 0.2 mm. In order to improve the adhesion of the coatings onto the substrates, at the end of the milling process, $Ti(iOPr)_4$ was added together with glacial acetic acid ($AcOH_{gl}$), the latter enabling its hydrolysis and long-term stability.[39] As shown by dynamic light scattering (DLS), the mTiA particles in mTiA pigment dispersions have average particle size of about 50 nm (Fig. 3).

Deposition of pigment coatings. Coatings were deposited on FTO glass (Pilkington, 14 Ω/) and conductive polymeric substrate (Solaronix, ITO PET 175 μm thickness; 60 Ω/□) by spin-coating techniques. By repeating the number of spinning deposition cycles (one cycle: spinning frequency = 1000 RPM, t = 40 s) thickness of the deposited TiO_2 coatings was varied from 100 nm (1x spinning) up to 400 nm (4x spinning) (Table 1). Also dip-coating deposition technique was used giving reproducible results in terms of coating thickness, morphology and pigment particle distribution. As regards our experiences with the deposition of $Ni_{1-x}O$,[17,18] and sol-gel spectrally selective paint coatings,[11] the corresponding TiO_2 dispersions were suitable also for continuous deposition via the coil-coating technique.

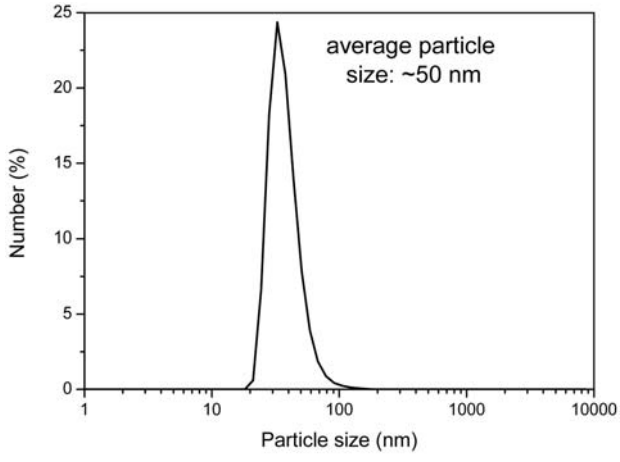

Fig. 3. Average particle size of particle aggregates in mTiA dispersion obtained from the DLS measurements was ~50 nm.

Table 1. Titania mTiA pigment coatings on FTO glass and ITO PET foil made from mTiA dispersions prepared with and without trisilanol-POSS dispersant and dispersions prepared from TiInfr and P25 TiO_2 powders. The size of milling beads was 0.1, 0.2 and 0.4 mm and the coatings were deposited various times (1 x, 2 x or 3 x).

TiO_2 coatings on FTO glass	Haze (%)	TT (%)	DT (%)
FTO glass	0.39	83.47	0.66
P25-02-1x[a]	5.11	80.92	4.59
TiInfr02-1x-P[b]	2.65	82.68	2.71
TiInfr02-02-1x	2.82	80.10	2.72
mTiA02-1x	2.76	83.52	2.83
mTiA02-2x	4.68	82.29	4.35
mTiA02-3x	5.93	81.40	5.30
mTiA01-1x-P	5.17	81.43	5.05
mTiA02-1x-P	1.68	83.36	5.01
mTiA04-1x-P	4.95	83.40	4.46
TiO_2 coatings on ITO PET plastic foil	**Haze (%)**	**TT (%)**	**DT (%)**
ITO PET	1.09	79.11	1.26
P25 - 2x	14.51	81.68	12.35
TiInfr02- 2x	12.80	81.69	10.99
TiInfr02-2x-P	14.26	81.22	12.19
mTiA02-2x	15.42	81.57	13.18
mTiA02-2x-P	16.83	82.96	14.57

[a,b] – Numbers 01, 02 and 04 in the names refers to the size of milling beads, letter P at the end of the name refers to the trisilanol POSS. 1x, 2x and 3x indicates the number of deposited layers.

Preparation of lithium conducting sol-gel electrolyte. An organic-inorganic hybrid on the basis of PEO chains and ethoxysilyl groups, classified as bis-end capped urethanosil (urethane -NH-C(=O)-O- bond instead of urea one), i.e. bis N-triethoxysilyl propylcarbamatoil PEO 400 (PEOCS)[49] was prepared by a reaction of 3-isocyanatopropyl-triethoxysilane with an equimolar amount of polyethylene glycol 400 (PEO 400) in tetrahydrofuran (THF). The reaction mixture was stirred together under reflux for 10 h. The THF was evaporated and the final product PEOCS was obtained. Glacial acetic acid ($AcOH_{gl}$) was chosen as the catalyst for the initiation of sol-gel processes, which inevitably leads to polycondensation of a bis end-capped alkoxysilane PEOCS precursor through a non-hydrolytic solvolysis route, liberating ester molecu-

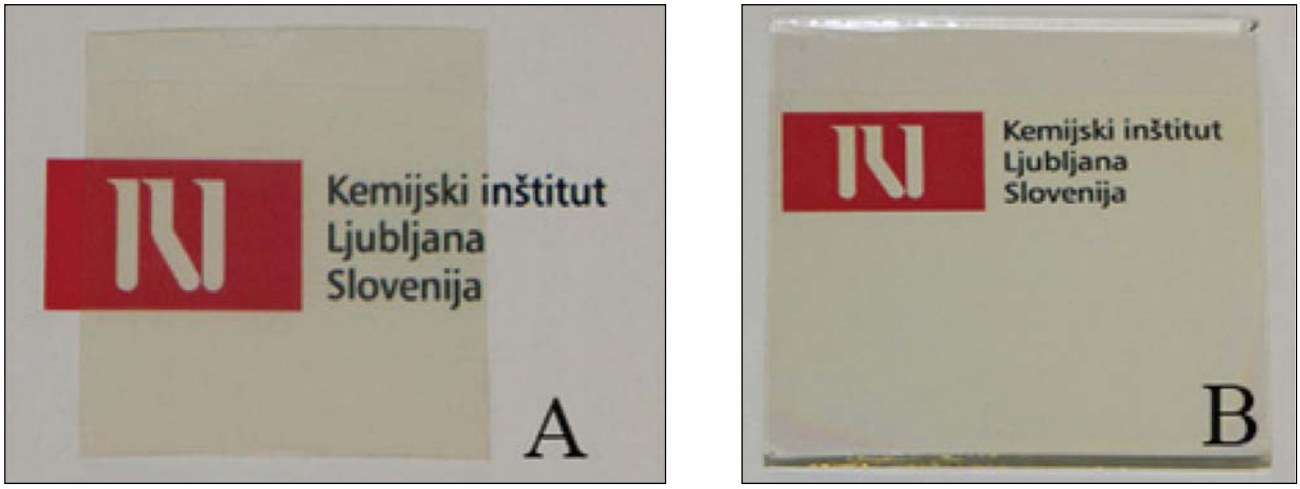

Fig. 4. mTiA02 pigment coatings obtained by 1x spin coating and thickness of about 150 nm deposited on ITO PET foil (A) and FTO glass (B) (for description see Table 1).

les.[51] In order to increase ionic conductivity, 3-methyl-1-(2,5,8,11,14,17,20,23,26,29,32-undecaoxypentatriacontan-35il)-1H imidazolium mesylate ($[PEO_{12}MeIm^+][OMs^-]$) ionic liquid was added in the sol-gel PEOCS network as co-solvent in molar ratio 1: 8 (PEOCS : ionic liquid). Addition of co-solvents has already been successfully suggested for electrolytes for lithium ion batteries.[52] The PEOCS hybrid and co-solvent were fully compatible and no segregation of phases was noted. The final electrolytes were obtained after dissolution of LiTFSI salt acting as a source of lithium ions.

Preparation of foil-based EC device. The EC device was made from mTiA02 and $Ni_{1-x}O$ pigment coatings combined with PEOCS/($[PEO_{12}MeIm^+][OMs^-]$)/LiTFSI/$AcOH_{gl}$ electrolyte. The electrolyte was spread on one of the electrodes (i.e. $Ni_{1-x}O$[17,18]) waited few minutes to dry and pressed together with another electrode (i.e. mTiA) until the electrolyte harden to a solid and transparent layer (~20 μm) gluing both halves of the EC device together. The performance of the foil-based EC device was evaluated by *in-situ* UV-Vis spectroelectrochemical measurements. The results showed moderate conductivity of electrolytes (approximately 10^{-4} S/cm) but the electrochemical window was quite large. The electrolytes exhibited excellent gluing properties. No sealing the flexible EC device was used.

2. 2. Instrumental

UV-Vis spectra of the pigment coatings on FTO glass and ITO PET foils were measured by a Perkin Elmer Lambda 900 UV-Vis spectrophotometer equipped with an integrating sphere. The optical quality of the coatings was estimated by determining transmission haze numbers (H in %), defined as the ratio of diffuse to total transmittance (DT/TT %) in the spectral range 380–780 nm following the ASTM test method D1003 as described previously.[17]

UV-Vis spectroelectrochemical properties of the coatings were characterized *in-situ* during potentiodynamic (cyclic voltammetry (CV) and chronocoulommetry (CC)) measurements on an Autolab PGSTAT 302N potentiostat-galvanostat. The coatings were examined in a 1 M $LiClO_4$/propylene carbonate (PC) electrolyte in a standard three electrode configuration consisting of the nanocrystalline TiO_2 coating on FTO glass (working electrode), a modified Ag/AgCl reference electrode and a platinum rod (counter electrode). The home-made spectroelectrochemical cell was mounted in an HP 8453A diode array spectrophotometer and the optical modulation of the coatings in the spectral range of 300 to 1100 nm recorded. CVs were measured between 0 and –1.7 V with a scan rate of 20 mV/s. CCs were used for coloration of coatings at –1.7 V (60 s) and bleaching at 0 V (60 s).

The specific conductivity of the sol-gel based electrolyte was measured on an Autolab PGSTAT 302N potentiostat-galvanostat with a FRA module in a Teflon cell between two Pt electrodes. The frequency range used for electrochemical impedance spectroscopy (EIS) was 10^5 to 0.01 Hz. The conductivity (σ in S/cm) was calculated according to the equation $\sigma = d/RA$, where R is the measured resistance obtained from the impedance plots, d the thickness and A the area of the sample between the Pt electrodes, respectively.

X-ray diffraction (XRD) analyses of surface modified m-TiA powders were done by means of a Siemens 5000D X-ray powder diffractometer equipped with graphite monochromatized Cu-Kα radiation (λ = 1.54178 Å). The scan speed was 10°/min, with a scan step of 0.02° of 2Θ.

3. Results and Discussion

3. 1. Properties of Coatings

Properties of coatings are given in Table 1, providing information about total visible transmittance (TT in %), total diffuse transmittance (DT in %) and the corresponding haze values (in %). Spectral total transmittance (TT (λ)) of pigment coatings and their haze changed with the coatings' thickness; thicker coatings prepared by repetitive spin-coating deposition (1x, 3x, 5x) showed decreasing transmittance values (Table 1), but scattering did not change much, which could be conceived from Fig. 5B, showing the values of haze (up to 6.0%) as a function of the milling conditions. The thickness varied also with regard to the applied milling beads, namely, mTiA01, mTiA02 and mTiA04 pigment coatings (all 1x-P (with trisilanol POSS)) were about 70, 150 and 260 nm thick, respectively. Expectedly, pigment coatings made of dispersions milled with the largest beads (0.4 mm) scattered more in the range of shorter wavelengths (Fig. 6) compared to the (TT in%) values of the coatings, which were made from dispersions milled with 0.1 mm beads. Haze was found to be the smallest for the coatings milled with 0.2 mm beads, which could be correlated with the coating surface roughness (R_s = 9.2 ± 2.0 nm),[21] which agreed also with surface topography of these pigment coatings showing homogeneously distributed particles. The size of the particles obtained was of about ~50 nm, which was also obtained from dynamic light scattering (DLS) (Fig. 3).

Inspection of results listed in Table 1 also revealed the influence of POSS dispersant on other titania coatings. Surprisingly, dispersant did not have pronounced effect on the haze of the TiInfr02 made with dispersant (TiInfr02-1x-P: 2.65%) and without it (TiInfr02-1x: 2.82%). P25 coating showed surprisingly high haze (5.11%), but the reasons for its high haze were not investigated further.

Haze values of the pigment coatings, which were deposited on ITO PET foils, drastically exceeded those determined for the same coatings on FTO glass (Table 1). We attributed this to the higher haze of ITO PET foil itself and also to the difference of the surface energy values of the foil and FTO glass, leading to different wetting and concurrently higher thickness of deposited coatings on foils compared to glass.

To conclude, mTiA pigment coatings did not show haze as low as noted for bare FTO glass and ITO PET substrates, but the clear sight through the coatings was not significantly hampered. The main part of scattering arose at shorter wavelengths, but was decreased significantly when the coatings were assembled in EC device (see below). Coatings exhibited interferences, which indicated that their properties closely resembled optical coatings.

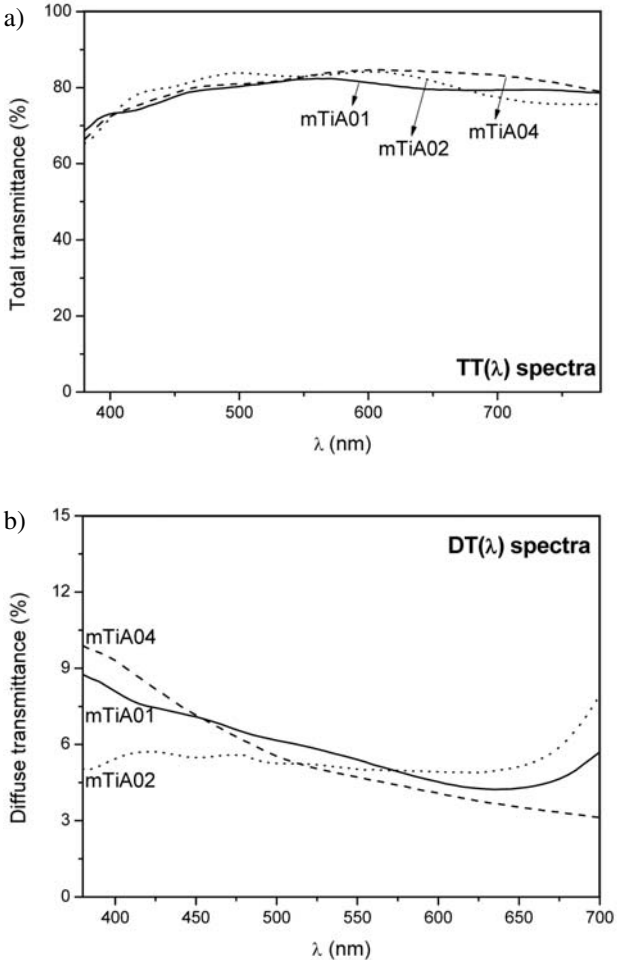

Fig. 5. Total (TT(λ)) (A) and diffuse (DT(λ)) (B) transmission spectra of mTiA01, mTiA02 and mTiA04 pigment coatings deposited on FTO glass and measured in air prepared under the same spin-coating conditions (all 1x-P (with trisilanol POSS)) (for description see Table 1).

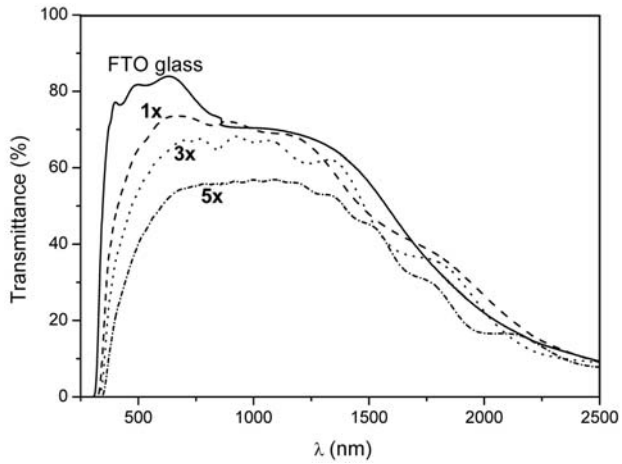

Fig. 6. Total transmittance (TT(λ)) spectra of mTiA pigment coatings prepared from trisilanol POSS/mTiA04 pigment dispersion milled with 0. 4 mm large zirconia beads deposited 1x, 3x and 5x by spin-coatings (for description see Table 1).

3. 2. Electrochemical Properties

3. 2. 1. Chronocoulometry (CC) and *in-situ* UV-Vis Spectroelectrochemical Measurement

Chronocoulometric (CC) and cyclic voltammetric (CV) measurements were carried out by immersing the mTiA pigment coatings (working electrode) in combination with a platinum counter electrode in a 1 M $LiClO_4$/PC electrolyte with an application of potential between 0 V and –1.7 V vs. Ag/AgCl reference electrode. The aim of the CV measurements was to determine the ability of the coatings to reversibly intercalate and deintercalate lithium ions, while the corresponding ion storage capacity (in mC/cm^2) was defined as the lithium ions inserted per unit active area of the coating using CC technique.

The CC measurements of the mTiA pigment coatings obtained by milling the pigment with different beads' size and with trisilanol POSS dispersant (all 1x-P in Fig. 7) revealed, that the ion storage capacity was higher for the mTiA04 than for other two pigment coatings (Fig. 7A). However, for all coatings, intercalation was higher than extraction (Fig. 7A), reaching for the mTiA04 coatings –32.1/+24.6 mC/cm^2. The corresponding ion storage capacity was higher than those of sol-gel amorphous or crystalline films by at least 2–3 times,[53] but still smaller compared to the heat-treated slip-casted coatings i.e., ~60 mC/cm.[25] Expectedly, colouring/bleaching changes increased with the coating thickness as a consequence of using different size of the milling beads, reaching up to ΔT 50% (λ = 800 nm) (Fig. 7B). Coloration efficiency (η in cm^2/C) varied accordingly, being the highest at larger wavelengths (Fig. 7B). Pigment coatings having different thicknesses, exhibited the same wavelength dependent η values suggesting that the insertion/extraction reactions proceeded throughout the whole coating thickness. Coloration efficiencies of pigment coatings were not exceptional for titania thin films and coatings as already reviewed by Sorar et al.[41]

EC effect was determined also for the pigment coatings, which were deposited on ITO PET substrate. The

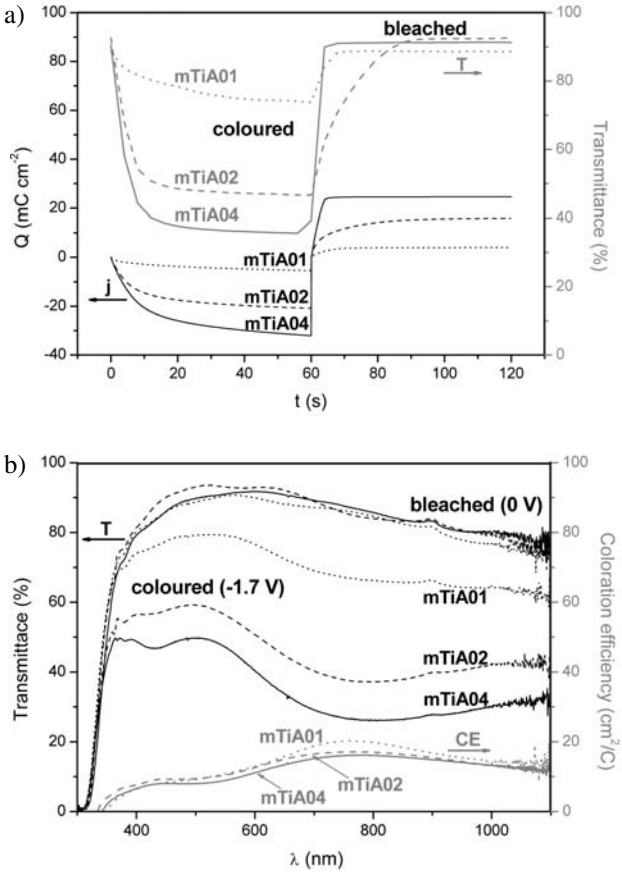

Fig. 7. *In-situ* UV-Vis spectroelectrochemical changes of mTiA01, mTiA02 and mTiA04 pigment coatings deposited by single spin-coating deposition on FTO glass, during CC colouring at –1.7 V (60 s) and bleaching at 0 V (60 s): A) CC curves and monochromatic transmittance changes at λ = 634 nm and B) UV-Vis spectra of coloured/bleached coatings with coloration efficiency as a function of wavelength (for description see Table 1).

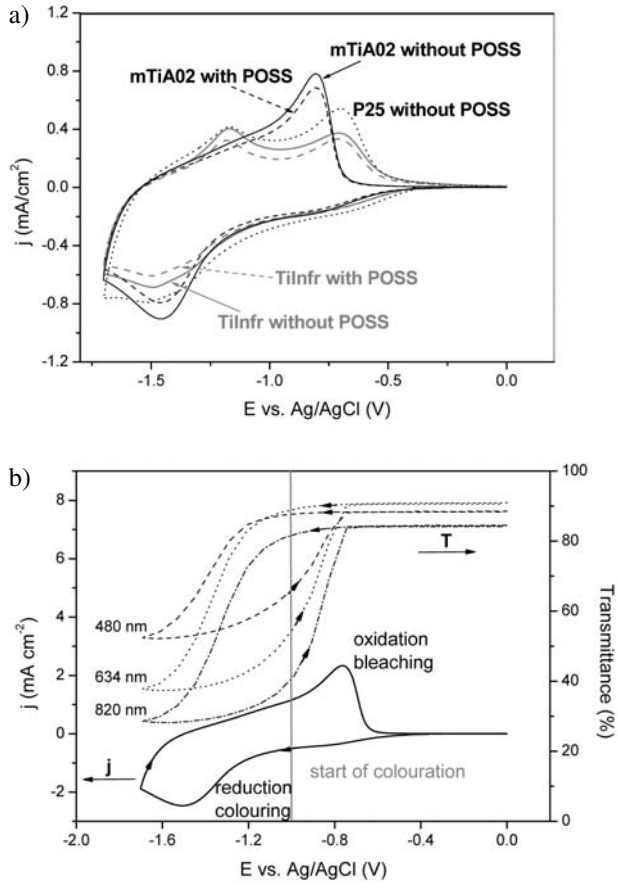

Fig. 8. *In-situ* UV-Vis spectroelectrochemical changes of mTiA02-2x-P pigment coating (see Table 1) deposited by two spinning cycles on ITO PET foil during CC colouring at –1.7 V (60 s) and bleaching at 0 V (60 s): A) CC curves and B) transmittance change during CC measurement.

mTiA02 pigment coatings were selected (Fig. 8) showing Q_{ins} ~ –47 mC/cm^2 and Q_{ext} ~ 38 mC/cm^2, inferring somewhat larger ion charging reversibility as noted for the same coatings deposited on FTO glass. EC effect was quite high reaching 70% at λ = 634 nm and dropped to 65% at λ = 480 nm, while the coloration efficiency was at the same wavelengths of about 10.7 cm^2/C, i.e. comparable to the values obtained for coatings deposited on FTO glass. Consequently, the haze of the pigment coatings on ITO PET was relatively high (16.83%), which was explained by different spreading of the pigment dispersion on both substrates. Pigment coatings did not show high speeds of colouring and bleaching, which was estimated to be ~1 min.

3. 2. 2. Cycling Voltammetry and *in-situ* Spectroelectrochemical Measurements

CVs provide information about potentials, at which oxidation and reduction reactions take place, enabling the distinction between the interacting sites of lithium ions and electrons as a function of materials' properties, i.e. size of crystallites, surface functionalization, porosity of coatings and their morphologies. In addition, from the variations of the current density of peaks obtained at various scan rates, information about the diffusion processes of intercalation species in the coatings can be obtained. The Randles-Sevčik equation is employed when the current peaks are proportional to the square root of the scan rate, but in the case that the current peaks show a linear dependence on the scan rate, the reactions are not diffusion-limited but rather surface reactions occur. This approach has been employed for confirmation of the surface charging of the $Ni_{1-x}O$ aggregates in the corresponding pigment coatings also prepared as "electrochromic paints".[17,18]

Effect of trisilanol POSS dispersant on CVs of the mTiA, TiInfr and P 25 pigment coatings, prepared with and without trisilanol POSS dispersant is shown in Fig. 9A. Inspections of the corresponding CVs revealed that dispersant did not have pronounced effect on the current densities of mTiA and TiInfr pigment coatings, but only slightly diminished the corresponding current density values. This was expected because trisilanol POSS interacted with the surface of the pigment aggregates screening the interacting sites and decreasing the extent of the insertion/extraction reactions.

The most apparent difference was observed in the shape of the CVs, which were quite different for the mTiA and TiInfr pigment coatings, the latter being nearly identical to the CV of the P25 pigment coatings, both also similar to the CV of the anodic spark-deposited pigment coatings.[24]. In the contrary, CVs of the TiInfr and P25 coatings resembled CVs of titania heat-treated thin films, deposited from colloidal solutions,[22,23,48,54–57]

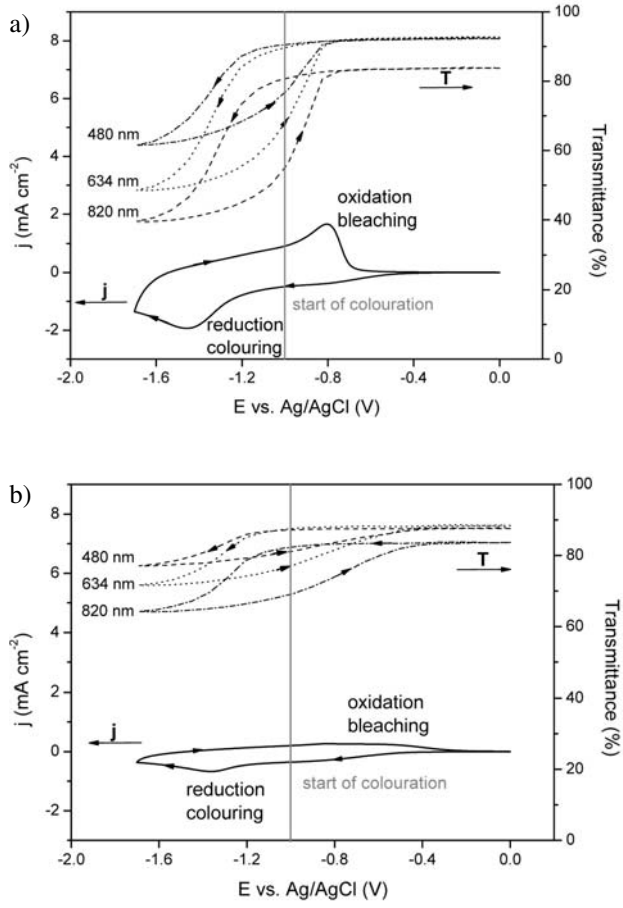

Fig. 9. A) Cyclic voltammograms of mTiA, TiInfr (for both: with and without dispersant) and P25 pigment coatings. *In-situ* UV-Vis spectroelectrochemical changes of the mTiA coatings: B) mTiA04, C) mTiA02 and D) mTiA01 (all 1x-P) (for description see Table 1). Start of colouration is indicated by grey vertical lines (see Figs. 9B-D).

heat-treated slip casted pigment coatings[25] and even titania thin films deposited with layer-by-layer deposition technique.[58]

The onset of colouring as function of applied potential was obtained from the *in-situ* UV-Vis spectroelectrochemical measurements, presented together with the CVs of the corresponding pigment coatings in Figs. 9B-D. Inspection of results revealed that CVs of the mTiA04, mTiA02 and mTiA01 pigment coatings were not the same, indicating the change of the interaction sites due to the size of the aggregates formed due to the different milling procedure. As expected, mTiA01 coatings (Fig. 9D) showed blurred peaks in the CVs, contrasting well-defined current density peaks in the CVs of the mTiA02 and mTiA04 pigment coatings (Fig. 9B, C). In this regards, the CVs of the mTiA01 coatings resembled CVs of the titania thin films prepared from the sol-gel precursor and heat-treated at 300 °C having also ill-defined crystallinity.[53] The same thin sol-gel films heat-treated at 560 °C have exhibited additional cathodic current peak at –0.86 V

vs. Ag/AgCl observed also as a weak and broad peak in CVs of the mTiA01 pigment coating (Fig. 8D). The corresponding cathodic peak has been attributed by Verma and Agnihotry,[53] to the presence of additional sites stemming from the crystallinity of the sintered sol-gel coatings. By analogy with the sol-gel sintered TiO_2 (anatase) thin films, the weak peak observed at –0.83 to –0.94 V was also attributed to the mTiA crystalline aggregates present in the pigment coatings (Fig. 8D).

In order to explain observed similarities between the mTiA01 and sol-gel amorphous and crystalline thin films[53], the mTiA02 pigment dispersion was milled 1 h more and the corresponding CVs were recorded (Fig. 10A). Comparison of CVs depicted in Fig. 9D and Fig. 10A showed, that the anodic peak at –0.83 to –0.94 V, which was seen in the CV of the mTiA01 coating (Fig. 9D) became observable also at ~0.94 V in the CV of the mTiA02 obtained by longer milling (Fig. 10A), mainly with low scan rates. Both described CVs showed smeared anodic current response between –0.6 V and –0.3 V (Fig. 9D, 10A).

Cathodic current peak at –0.83 to –0.94 V, observed also by Verma and Agnihotry,[53] for the crystalline sol-gel EC anatase films, we attributed to the electrochemical activity of the surface of mTiA aggregates. The corresponding cathodic peak was difficult to fit with sufficient reliability because its intensity was low and further lowered with increased scan rates, i.e. it vanished already at scan rates higher than 6 mV/s. On the contrary, cathodic peak at –1.5 V and its counterpart in a reverse scan at –0.8 V showed quite good linear dependence vs. square root of scan rates (Fig. 10B) albeit at low scan rates the deviation from the linearity was noticed. Fast vanishing of the cathodic current peak at –0.83 to –0.94 V strongly suggested the existence of some electrochemically active surface sites, contrasting start of coloration for the main cathodic current peak at ~1.5 V, which is in agreement with other reports.[22,23,25,48,55–59]

To conclude, according to expectations, the insertion/extraction of electrons and lithium ions represented the main mechanism of electrochromic effect of mTiA pigment coatings,[1] but their CV response reflected that the degree of the pigment aggregates was achieved for dispersions by variation of the milling procedures. Pigment coatings also showed quick saturation of specific sites of the crystalline aggregates, but the unquestionable confirmation of the statement that they were attributed to the low lying electron states, which are electrochromically deaf[24,59] was not obtained. EC effect also depended on the extent of milling indirectly through the coating thickness, being higher for coatings milled with larger zirconia beads.

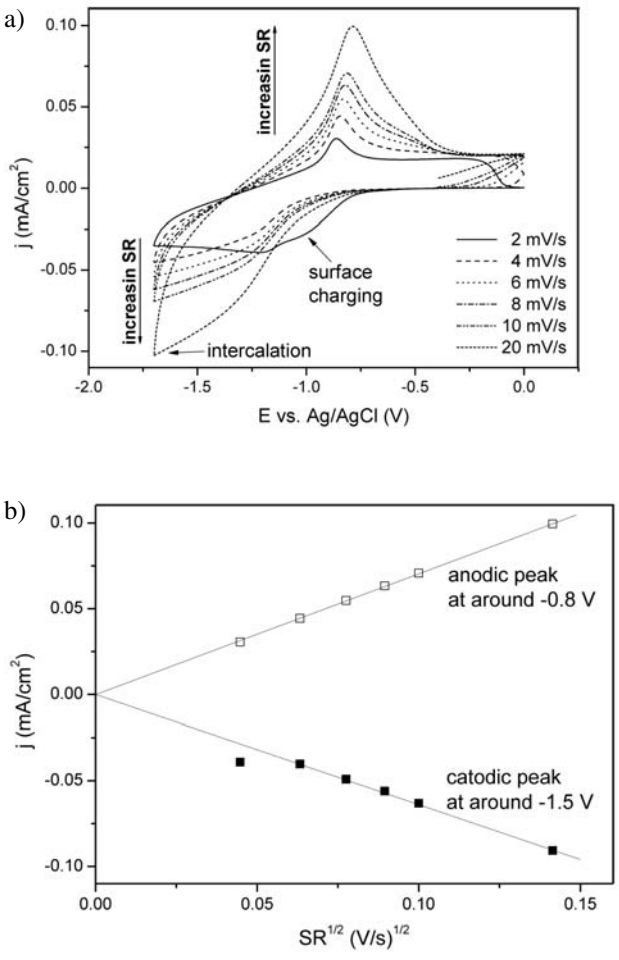

Fig. 10. Cyclic voltammograms of the mTiA02 coating made with 0.2 mm zirconia beads (longer time of milling, 2 h) and with trisilanol POSS dispersant at different scan rates: A) CVs, B) peak current densities vs. square root of scan rates. Current peaks (A) revealing surface charging (–0.83 to –0.94 V) and the start of the intercalation reactions (–1.5 V) are also indicated.

3. 3. Flexible EC Device

Flexible EC device was assembled from mTiA02 and $Ni_{1-x}O$[17,18] pigment coatings deposited on ITO PET foils and produced as "electrochromic paint". $Ni_{1-x}O$ pigment coating was 500–600 nm thick and its haze was 10.8%, while the corresponding TT and DT values were 52.9 and 6.1%, respectively, and the inserted and extracted charge (Q_a/Q_c) was +15.2/–13.1 mC/cm^2. The coloration efficiency of the $Ni_{1-x}O$ pigmented coating was 54.6 cm^2/C (λ = 480 nm). Other details about the $Ni_{1-x}O$ pigmented coatings can be obtained from ref.[17,18] Since $Ni_{1-x}O$ is anodic material and mTiA cathodic one, in EC device they coloured simultaneously at negative and bleached at positive potentials, contributing to the enhanced electrochromic effect (Fig. 11). When charge capacities and coloration efficiencies match, the foil based EC device provides neutral colouring shown below.

The EC device was assembled by application of PEOCS/LiTFSI/$PEO_{12}MeIm^+OMs^-$/$AcOH_{gl}$ electrolyte, having the conductivity of 2×10^{-4} S/cm. Electrochemical

and optical response of the EC device was obtained when potential was swept from +2.2 to –2 V as shown in Fig. 11A. The variation of transmittance at λ = 634 nm with the chronocoulometric application of –2 V for colouring and 2.2 V for bleaching is shown in Fig. 11B, while the corresponding spectral response of EC foil-based device is depicted in Fig. 11C.

Inspection of results revealed, that the EC device showed the properties of both EC coatings, which we inferred from the presence of current peaks of mTiA02 at cathodic and $Ni_{1-x}O$ at anodic potentials (Fig. 11A). Moreover, the transmittance of device in its initial state was lower compared to the transmittance obtained when device was bleached. This we attributed to the substoichiometric $Ni_{1-x}O$ pigmented coating, which was not completely transparent in its initial state because of the presence of Ni^{+2}/Ni^{+3} redox couple.[17,18] Differences in the CVs attributed to the $Ni_{1-x}O$ at positive and mTiA02 at negative potentials indicated that the EC device was not perfectly balanced, which we attributed to the differences in the coating's thickness being 600 nm for $Ni_{1-x}O$ and 150 nm for mTiA pigment coatings affecting the inserted/extracted charges. EC device also showed fast bleaching (10–20 s) but the speed of colouring was rather small. It seemed that even after 1 min of charging the maximal colouring was not yet achieved (Fig. 11B).

Spectral response of transmitted light is important practical issue regarding construction of EC device with neutral-tint coloration. Coloration of foil-based EC device was expressed with the colour coordinates in L*a*b* colour space (Fig. 11D, Table 2).

It is evident that the blue coloration (negative b* values) of mTiA pigmented coating was overwhelmed with the brown coloration of $Ni_{1-x}O$ pigmented coating (positi-

Table 2. Lightness L* of the constructed foil-based EC device.

pigmented coating / EC device	L^*_{col}	L^*_{bl}
$Ni_{1-x}O$ on ITO PET	61.5	92.6
mTiA02 on ITO PET	61.7	96.2
flexible EC device	47.8	76.3

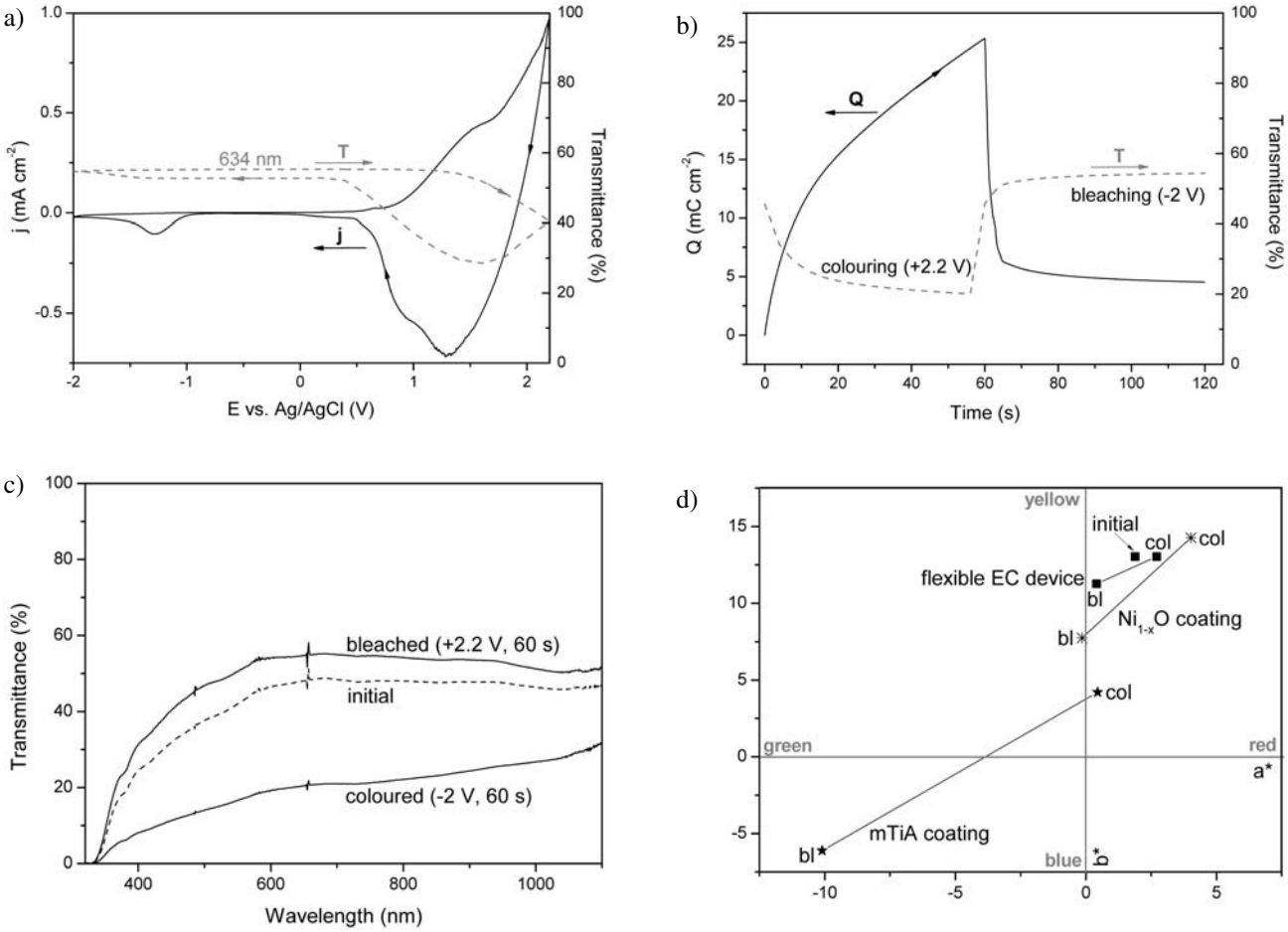

Fig. 11. *In-situ* UV-Vis spectroelectrochemical measurements of mTiA02/sol-gel electrolyte/$Ni_{1-x}O$ flexible EC device: A) CV curve with monochromatic transmittance response at 634 nm, B) CC curve with transmittance response at 634 nm, C) UV-Vis spectra and D) a* and b* colour coordinates.

ve a*, b* values). The EC device in bleached (a* = 0.4, b* = 11.3) and coloured (a* = 2.7, b* = 13.0) state revealed positive a* and b* values, the increase in a* during colouring of device indicating the tendency towards brown coloration. The initial colour of the foil-based EC device was closer to the a*,b* values of the device in coloured state, since the substoichiometric $Ni_{1-x}O$ was initially brownish as a consequence of the presence of Ni^{3+} ions.[17,18] Lightness L* increased from 47.8 (coloured) to 76.3 for the bleached state due to its higher transmittance. Contrary to mTiA/sol-gel electrolyte/$Ni_{1-x}O$ device the already reported flexible EC device with the same electrolyte and PEDOT and V-oxide electrodes[50] showed optical modulation from dark blue area (a* = 1.1, b* = –29.3) to the brighter blue area (a* = 8.8, b* = 7.4) due to the high thickness of blue-colouring PEDOT (800 nm). It seemed that by using inorganic EC materials, neutral-tint EC device is easier to be made compared to the EC device with mixed organic (PEDOT) and inorganic $Ni_{1-x}O$ EC coatings.

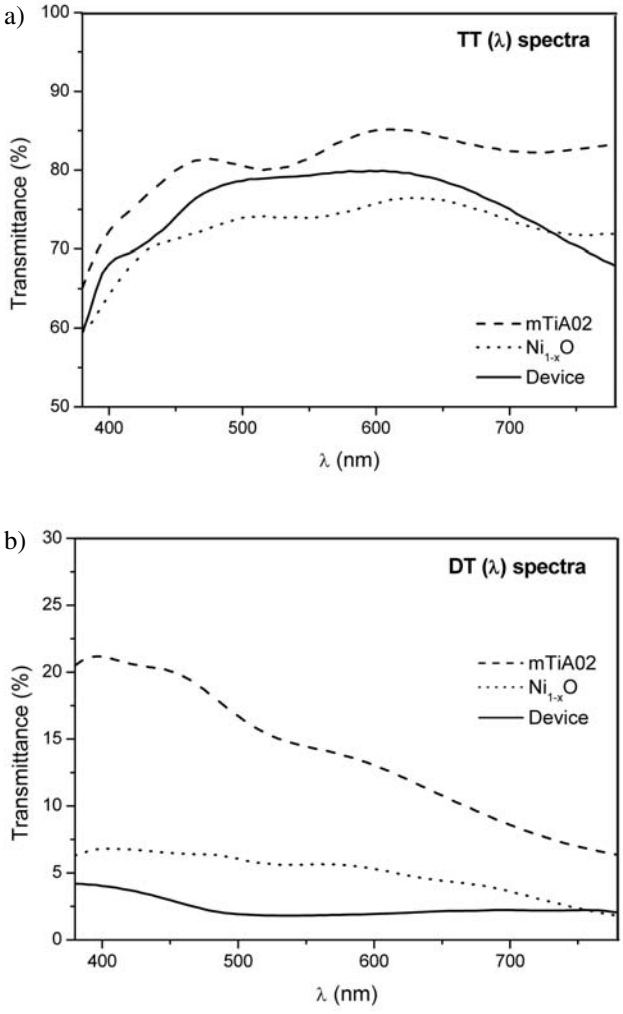

Fig. 12. Total (TT(λ)) (A) and diffuse (DT(λ)) (B) transmission spectra of mTiA02 and $Ni_{1-x}O$ pigment coatings and, mTiA02/sol-gel electrolyte/$Ni_{1-x}O$ flexible EC device.

Inspection of haze values revealed that even though the haze of the individual components was 10.8% ($Ni_{1-x}O$) and 16.8% (mTiA02), the haze value of the complete flexible EC device was just 6.3% (Fig. 12). This indicated positive effect of the semi-solid (or gel) electrolyte whose refractive index was much higher than air, which compensated the surface roughness of both EC pigmented coatings. Obviously, the electrolyte perfectly wetted the electrodes by entering within the surface pores of the coatings.

4. Conclusions

The main advantage of depositing electrochromic pigment coatings from pigment dispersions, i.e. "electrochromic paints", lies in the fact, that EC pigment coatings can be deposited at temperatures, which were compatible with temperature stability of plastic foils (~150 °C).

In addition, using this procedure, many different inorganic electrochromics,[1] which are otherwise difficult to be deposited in the form of thin films at low temperatures, can be used. Thus, the described procedure started from the synthesis of electrochromic pigment, which was in the next stage milled with zirconia beads of different size in the butanol/trisilanol POSS mixture, until the particle aggregates reached the size of 30–50 nm. A small amount of added $Ti(iOPr)_4$ served as binder, which contributed to the mechanical integrity of the pigment coatings.

Results confirmed our expectations that the optical quality of the coatings, i.e. haze, depended on the duration of milling and the size of the zirconia beads. The process allowed the deposition of coatings with about 5% of haze and electrochromic transmittance changes of up to 60%. Coil-coating (R2R) deposition technique on ITO PET foils is preferred.

Trisilanol POSS dispersant, which served for dispersing mTiA pigment in solvent, did not hamper electrochromic efficiency indicating sufficient porosity of the trisilanol POSS layer to allow the transfer of lithium ions across the dispersant layer.

The EC effect of cathodic mTiA electrochromic material is a multifaceted problem, which was affected by many variables: the chemical composition of pre-prepared EC pigment, its preparation route, the coatings' porosity and surface structure. It was shown, that the cyclic voltammetry peaks of mTiA coatings prepared from pigment dispersions milled with different zirconia beads and milling times can differ to some extent. The observed EC effect of the mTiA pigment coatings depended on the extent of milling; larger zirconia beads provided thicker coatings and correspondingly stronger colouring/bleaching changes. However, coloration efficiency remained equal for all three grades of mTiA pigment coatings, from which we inferred, that all three pigment coatings exhibited similar access for lithium ions throughout their physical thickness.

All mTiA pigment coatings showed electrochemical activation period. After few initial potential cycles, weak cathodic peak at –0.83 to –0.94 V disappeared, which we tentatively ascribed to the interactions with the electrochemically active surface sites. As expected, these sites did not bring about EC effect, which started at potential region where the strongest CV peak at –1.3 to –1.6 V was observed. mTiA pigment coatings behave as typical cathodic electrochromic material.

CVs response of TiInrf and P25 pigment coatings differed as regards the CVs of mTiA coatings, which was attributed to the presence of additional electrochemical sites.

Foil-based EC devices showed reversible and persistent EC effect (up to 200 cycles). As expected, haze of the EC devices was lower compared to the haze of the individual pigment coatings, which we attributed to the effect of the electrolyte, filling surface defects and surface roughness of the mTiA and $Ni_{1-x}O$ pigment coating electrodes.

5. Highlights

– Electrochromic pigment coatings were deposited from nanodispersions of anatase
– Trisilanol POSS was used as dispersant for anatase pigment dispersions
– Low temperature TiO_2 pigment coatings on conducting polymeric substrates
– Flexible EC device was constructed from TiO_2 and $Ni_{1-x}O$ pigment coatings

6. Acknowledgements

The research leading to these results has received funding from the European Community's Seventh Framework Programme (FP7) under Grant agreement no. 200431 (INNOSHADE), from CO-NOT, Centre of Excellence for Low-Carbon Technologies and Programme P1-0030 (Slovenian Research Agency). Acknowledgement to Dr. Marija Čolović for synthesis of electrolyte precursors and Doc. dr. Ivan Jerman for help in preparation of pigment dispersions.

7. References

1. C. G. Granqvist, Handbook of inorganic electrochromic materials, Elsevier, Amsterdam, **1995**, pp. 633.
2. C. G. Granqvist, *Sol. Energy Mater. Sol. Cells* **2008**, *92*, 203–208.
3. R. Baetens, B. P. Jelle, A. Gustavsen, *Sol. Energy Mater. Sol. Cells* **2010**, *94*, 87–105.
4. M. C. Choi, Y. Kim, C. S. Ha, *Prog. Polym. Sci.* **2008**, *33*, 581–630.
5. C. G. Granqvist, A. Azens, P. Heszier, L. B. Kish, L. Osterlund, *Sol. Energy Mater. Sol. Cells* **2007**, *91*, 355–365.
6. E. J. Widjaja, G. Delporte, F. Vandevelde, B. Vanterwyngen, *Sol. Energy Mater. Sol. Cells* **2008**, *92*, 97–100.
7. Skip Scriven, L.E., in: M. A. Galan, E. M. del Valle (Eds.), Chemical Engineering, John Wiley & Sons, Ltd., **2005**, Ch. 9, pp. 229–266.
8. C. Brigouleix, P. Topart, E. Bruneton, F. Sybary, G. Nouhant, G. Campet, *Electrochim. Acta* **2001**, *46*, 1931–1936.
9. C. M. Lampert, *Sol. Energy Mater. Sol. Cells* **2003**, *76*, 489–499.
10. C. M. Lampert, *Displays* **2004**, *25*, 165–165.
11. I. Jerman, M. Mihelčič, M. Koželj, B. Orel, Sol-gel based spectrally selective solar absorber coatings and the process for producing said coatings, WO patent number 2013158049 A1, date of patent October 24, **2013**.
12. I. Jerman, M. Koželj, B. Orel, *Sol. Energy Mater. Sol. Cells* **2010**, *94*, 232–245.
13. I. Jerman, M. Mihelčič, D. Verhovšek, J. Kovač, B. Orel, *Sol. Energy Mater. Sol. Cells* **2011**, *95*, 423–431.
14. R. Kunič, M. Mihelčič, B. Orel, L. Slemenik Perše, B. Bizjak, J. Kovač, S. Brunold, *Sol. Energy Mater. Sol. Cells* **2011**, *95*, 2965–2975.
15. K. Vojisavljević, B. Malič, M. Senna, S. Drnovšek, M. Kosec, *J. Eur. Ceram. Soc.* **2013**, *33*, 3231–3241.
16. F. Švegl, A. Šurca Vuk, M. Hajzeri, L. Slemenik Perše, B. Orel, *Sol. Energy Mater. Sol. Cells* **2012**, *99*, 14–25.
17. M. Mihelčič, I. Jerman, F. Švegl, A. Šurca Vuk, L. Slemenik Perše, J. Kovač, B. Orel, U. Posset, *Sol. Energy Mater. Sol. Cells* **2012**, *107*, 175–187.
18. M. Mihelčič, A. Šurca Vuk, I. Jerman, B. Orel, F. Švegl, H. Moulki, C. Faure, G. Campet, A. Rougier, *Sol. Energy Mater. Sol. Cells* **2014**, *120*, 116–130.
19. H. Moulki, C. Faure, M. Mihelčič, A. Šurca Vuk, F. Švegl, B. Orel, G. Campet, M. Alfredsson, A. V. Chadwick, D. Gianolio, A. Rougier, *Thin Solid Films* **2014**, *553*, 63–66.
20. D. Verhovšek, N. Veronovski, U. Lavrenčič Štangar, M. Kete, K. Žagar, M. Čeh, *Int. J. Photoenergy* **2012**, ID 329796, 10 pages.
21. M. Mihelčič, I. Jerman, B. Orel, *Prog. Org. Coat.* **2013**, *76*, 1752–1755.
22. T. Ohzuku, T. Hirai, *Electrochim. Acta* **1982**, *27*, 1263–1266.
23. T. Ohzuku, T. Kodama, T. Hirai, *J. Power Sources* **1985**, *14*, 153–166.
24. D. Reinhardt, S. Krieck, S. Meyer, *Electrochim. Acta* **2006**, *52*, 825–830.
25. N. Nang Dinh, N. M. Quyen, D. N. Chung, M. Yikova, V. V. Truong, *Sol. Energy Mater. Sol. Cells* **2011**, *95*, 618–623.
26. R. Cinnsealach, R. Boschloo, S. N. Rao, D. Fitzmaurice, *Sol. Energy Mater. Sol. Cells* **1998**, *55*, 215–223.
27. U. Bach, D. Corr, D. Lupo, F. Pichot, M. Ryan, *Adv. Mater.* **2002**, *14*, 845–848.
28. A. Hagfeldt, G. Boschloo, L. Sun, L. Kloo, H. Pettersson, *Chem. Rev.* **2010**, *110*, 6595–6663.
29. G. Leftheriotis, G. Syrrokostas, P. Yianoulis, *Sol. Energy Mater. Sol. Cells* **2010**, *94*, 2304–2313.

30. Baudry, P., A. C. M. Rodriguez, M. A. Aegerter, L. O. Bulhoes, J. Non-Cryst. Solids **1990**, *121*, 319–322.
31. U. Lavrenčič Štanger, B. Orel, I. Grabec Švegl, B. Ogorevc, K. Kalcher, *Sol. Energy Mater. Sol. Cells* **1993**, *31*, 171–185.
32. U. Lavrenčič Štanger, B. Orel, I. Grabec Švegl, B. Ogorevc, Acta Chim. Slov. **1994**, *41*, 39–64.
33. T. Seike, J. Nagai, *Sol. Energy Mater.* **1991**, *22*, 107–117.
34. S. F. Cogan, E. J. Anderson, T. D. Plante, R. D. Rauh, Materials and Devices In Electrochromic Window Development, in: Proceedings of SPIE – The International Society for Optical Engineering **1985**, *562*, 23–31.
35. M. Kitao, Y. Oshima, K. Urabe, *Jap. J. Appl. Phys.* **1997**, *36*, 4423–4426.
36. A. Gutarra, A. Azens, B. Stjerna, C. G. Granqvist, *Appl. Phys. Lett.* **1994**, *64*, 1604–1606.
37. K. Lee, D. Kim, S. Berger, R. Kirchgeorg, P. Schmuki, *J. Mater. Chem.* **2012**, *22*, 9821–9825.
38. T. J. Richardon, M. D. Rubin, *Electrochim. Acta* **2001**, *46*, 2119–2123.
39. S. Doeuff, C. Sanchez, *Comptes Rendus del'Academie des Sciences, Série 2*, **1989**, *309*, 531–534.
40. T. Ivanova, A. Harizanova, T. Koutzarova, N. Krins, B. Vertruyen, *Mater. Sci. Engin. B* **2009**, *165*, 212–216.
41. I. Sorar, E. Pehlivan, G. A. Niklasson, C. G. Granqvist, *Sol. Energy Mater. Sol. Cells* **2013**, *115*, 172–180.
42. J. Livage, D. Ganguli, *Sol. Energy Mater. Sol. Cells* **2001**, *68*, 365–381.
43. Ozer, N., *Thin Solid Films* **1992**, *214*, 17–24.
44. N. Ozer, F. Tepehan, N. Bozkurt, *Thin Solid Films* **1992**, *219*, 193–198.
45. P. A. Gillet, J. L. Fourquet, O. Bohnke, *Mater. Res. Bull.* **1992**, *27*, 1145–1152.
46. T. Ivanova, A. Harizanova, *Mater. Res. Bull.* **2005**, *40*, 411–419.
47. R. van de Krol, A. Goossens, J. Schoonman, *J. Phys. Chem. B* **1999**, *103*, 7151–7159.
48. I. B. Pehlivan, R. Marsal, E. Pehlivan, E. L. Runnerstrom, D. J. Milliron, C. G. Granqvist, G. A. Niklasson, *Sol. Energy Mater. Sol. Cells*, http://dx.doi.org/10.1016/j.solmat.2013.06.010.
49. V. de Zea Bermudez, L Alcácer, J. L Acosta, E Moraleset, *Solid State Ionics* **1999**, *116*, 197–209.
50. M. Hajzeri, A. Šurca Vuk, L. Slemenik Perše, M. Čolović, B. Herbig, U. Posset, M. Kržmanc, B. Orel, *Sol. Energy Mater. Sol. Cells* **2012**, *99*, 62–72.
51. B. Orel, R. Ješe, A. Vilčnik, U. Lavrenčič Štangar, *J. Sol-Gel Sci. Technol.* **2005**, *34*, 251–265.
52. Y. Matsuo, K. Fumita, T. Fukutsaka, Y. Sugie, H. Koyama, K. Inoue, *J. Power Sources* **2003**, *119–121*, 373–377.
53. A. Verma, S. A. Agnihotry, *Electrochim. Acta* **2007**, *52*, 2701–2709.
54. F. Cao, G. Oskam, P. C. Searson, J. M. Stipkala, T. A. Heimer, F. Farzad, G. J. Meyer, *J. Phys. Chem.* **1995**, *99*, 11974–11980.
55. M. Ottaviani, S. Panero, S. Morzilli, B. Scrosati, M. Lazzari, *Solid State Ionics* **1986**, *20*, 197–202.
56. G. Boschloo, D. Fitzmaurice, *J. Phys. Chem. B* **1999**, *103*, 7860–7868.
57. A. Hagfeldt, N. Vlachopoulos, M. Grätzel, *J. Electrochem. Soc.* **1994**, *141*, L82–L84.
58. T. Facci, F. Huguenin, *Langmuir* **2010**, *26*, 4489–4496.
59. M. Koelsch, S. Cassaignon, C. Ta Thank Minh, J.-F. Guillemoles, J.-P. Jolivet, *Thin Solid Films* **2004**, *451*, 86–92.

Povzetek

Tanke elektrokromne plasti smo naredili s sočasnim mletjem delcev mTiA agregatov (300 nm) s heptaizobutil trisilanol POSS (T_8 IB_7 $(OH)_3$ POSS), ki je deloval kot disperzant in dodatkom titanovega tetraizopropoksida (3–5 %) ter pigmentno disperzijo nanesli na FTO steklo in polimerne ITO PET folije in jih nato termično obdelali pri 150 °C.

Optično prepustnost in motnost prevlek smo določili na osnovi UV-Vis spektrov. Motnost prevlek na FTO steklu je znašala od 2 do 6 %, odvisno od debeline plasti. Elektrokromni učinek prevlek smo ocenili z elektrokemijsko interkalacijo/deinterkalacijo v 1 M LiClO4/PC elektrolitu. Rezultati so pokazali, da je optična modulacija odvisna od dolžine mletja in velikosti cirkonij-oksidnih kroglic, omogočili pa so tudi razlikovanje med površinskim nabijanjem mTiA delcev ter polnjenjem/praznenjem anataznih delcev.

mTiA pigmentne prevleke, ki smo jih nanesli na polimerne folije, smo uporabili v kombinaciji z $Ni_{1-x}O$ pigmentnimi prevlekami za izdelavo fleksibilnega elektrokromnega sklopa z novim gelskim elektrolitom in ionsko tekočino kot sotopilom.